Optimized electrode positions and stimulation patterns in head EIT

Yasin Mamatjan[1], Sujin Ahn[2], Tongin Oh[3] and Andy Adler[1]
[1] Systems and Computer Engineering, Carleton University, Ottawa, Canada
[2]School of Information & Communications, Gwangju Institute of Science and Technology, Korea
[3]Impedance Imaging Research Center, Kyung Hee University, Korea

***Abstract*—Electrical Impedance Tomography (EIT) has potential for imaging of the head to image cerebral edema and stroke, and to assist the EEG inverse problem. One key challenge is the low distinguishability of head EIT. In this paper, we develop a strategy to improve distinguishability by optimizing electrode configurations and stimulation and measurement patterns. In a hemispherical simulation phantom, electrode positions and patterns were evaluated for (i) 1-ring 16 electrodes, (ii) 2-ring equal number of electrodes, (iii) 3-ring electrode geometries and (iv) 10-20 system of EEG electrode configuration. A selected best case was experimentally evaluated using a KHU Mark2 EIT system and compatible saline phantom. The objective was to design an EIT electrode geometry and stimulation pattern to yield high SNR across a large region of interest within the head. Results show that multi-level electrode geometries produced higher distinguishability, especially the multi-layer 10-20 electrode configuration provides the highest distinguishability and best image reconstruction performance.**

I. Introduction

Electrical impedance tomography (EIT) is a non-invasive and non-ionizing imaging technology used for detecting and monitoring physiological changes inside a human body. In EIT, changes in electrical conductivity within a body are imaged using current injections and voltage readings consecutively via a set of electrodes arranged around a body of interest. One exciting possible application of EIT is acute stroke imaging since early detection of ischemic stroke is critical for a decision on the use of thrombolytic medication.

Most of the EIT systems have been designed as the Sheffield protocol with applied currents and voltage measurements on an adjacent pair of electrodes [1]. Recently, simulated brain imaging was conducted based on a limited protocol with ten stimulation and measurement patterns [2]. Spiral configuration with suboccipitalelectrodes with current injection $180^\circ + 120^\circ + 60^\circ$ gave the best image quality compared to images from several other protocols and had a localization error less than 10 % of head diameter. To use the practical EIT system for human head, there is a need for a systematic study and evaluation for optimizing sensitivity and increasing detectability by choosing good stimulation patterns and electrode placement strategies.

Our recent study on stimulation and measurement patterns in a single electrode plane of a cylindrical phantom suggested that the stimulation and measurement patterns separated radically by one electrode less than 180° as the optimal current pattern [3]. This also motivated us to further investigate multi-plane electrode placement in 3D hemispherical phantom particularly for the application to the head stimulation and EEG inverse problem, and evaluate it with a real EIT system.

To address this issue, we conducted 3D simulation study and experimental evaluation of selected electrode placement strategies. The objective is to compare and select such electrode geometry that the full ensemble of measurements provides high distinguishability. The electrode geometries studied in this paper were (i) the conventional 1-ring 16 electrodes, (ii) 2-ring with an equal number of electrodes (8 electrodes) for both layers, (iii) 3-ring electrodes, and (iv) international 10-20 system of EEG electrode placement (referred as 10-20 system), which was developed as a standardized electrode position on the scalp. Based on these results, we provide recommendations on optimal electrode placement, and best stimulation and measurement patterns for each electrode configurations for head EIT.

II. Methodology

We simulate and experimentally evaluate various single and multi-plane electrode geometries connected to a hemispherical phantom, and apply different stimulation and measurement patterns based on a set of simulation and measurement protocols. We aim to optimize electrode positions and stimulation patterns to improve sensitivity and distinguishability (SNR) in head EIT.

A. Simulation of head EIT

The EIDORS algorithm [4] was employed for simulating different electrode geometries and current patterns in Fig. 1. A hemispherical phantom was modelled for all the simulations in this study using Netgen. To reconstruct images, the EIT model has been reconfigured to calculate the sensitivity matrix by simulating current patterns and measuring signals from corresponding electrodes.

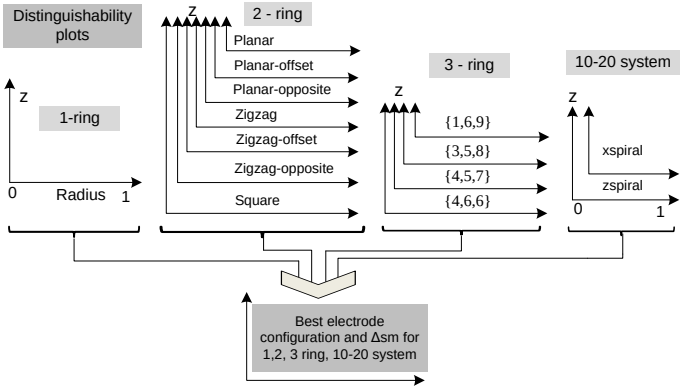

Fig. 1. A block diagram showing the general steps for selecting optimal electrode placement strategies from 1, 2, 3 ring electrodes and 10-20 system. Thus, we first compared the performance of single and multi-layer electrode geometries within each group (row 1), and then we selected the best electrode configuration from each group and made further cross-comparisons.

Phantom and target object: The hemispherical phantom has a height of 92 cm and radius of 90 cm. The hemispherical phantom was filled with a saline solution (conductivity of 0.176 Sm^{-1}) to a height of 90 cm.

Movement protocols: The target object used in our experiment is a sliced cubic carrot with a conductivity of 0.026 Sm^{-1} and side length of 16.2 cm. The object was moved to 6 positions from the center to the edge of the phantom in a radial direction (along Y axis) at the central plane at the positions of (0,0,51), (0,12,51), (0,24,51), (0,36,51), (0,48,51), and (0,60,51) where X,Y,Z axis are in cm. A normalized distances were used by dividing the distances with the height of saline solution filled in the hemispherical phantom (90 cm) and the central plane of the hemisphere was fixed to 51 cm with a normalized distance of 0.5667 (51/90).

Electrode geometries: The proposed electrode geometries were described below:

1-ring electrode placement: The hemispherical phantom was encircled by 1 plane 16 electrodes, which were positioned at equal intervals around the central plane (53 cm) of hemispherical phantom.

2-ring electrode placement: The 2-ring electrode geometry has an equal number of electrodes (8 electrodes) for both layers which include 7 electrode geometries such as Planar, Planar-offset, Planar-opposite, Zigzag, Zigzag-offset, Zigzag-opposite and Square electrode placement strategies as defined by [5].

3-ring electrode placement: We simulated electrode geometries placed around 3 layers with different number of electrodes on each plane such as $\{1,6,9\}, \{3,5,8\}, \{4,5,7\}, \{4,6,6\}$ for $\{$first, second and third$\}$ electrode layers.

10-20 system: Fig. 2 shows mapping 10-20 system to simulation electrode number using 16 electrodes. For 10-20 system, we considered typical two driving patterns as current injection direction on 10-20 system which were x-spiral and z-spiral. The x-spiral means that current was applied on the direction following the spiral centered at x-axis, also z-spiral was the spiral centered at z-axis.

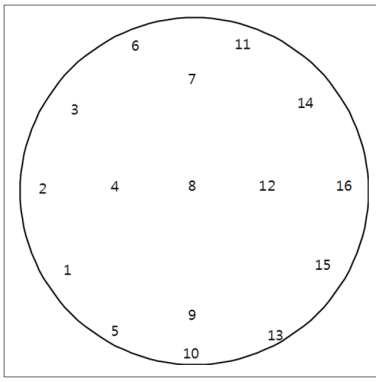

10-20 EEG System	Number
Fp1	6
Fp2	11
F3	3
Fz	7
F4	14
T7	2
C3	4
Cz	8
C4	12
T8	16
P3	1
Pz	9
P4	15
O1	5
Oz	10
O2	13

Fig. 2. 16 electrodes were mapped to the 10-20 system.

Stimulation patterns: Electric current was fed consecutively through different available electrode pairs and the corresponding voltage measured consecutively by all remaining electrode pairs. Stimulation (Δ_s=1,...,8) and measurement (Δ_m=1,...,8) patterns are defined by the distance between the two active electrodes for the stimulation or measurement function, and thus formed different stimulation and measurement patterns (Δ_{sm}) for each electrode geometry.

B. Experimental design and EIT measurement system

Induced voltages were measured between adjacent channels only due to the hardware connection. However, we could produce difference voltages between other electrode pairs by applying superposition principle. The experiment was performed at a single frequency of 10 kHz and 1 mA of current was injected. We recorded data with and without the cubic target for each case.

KHU Mark2 (Kyung Hee University, Korea) EIT system includes 16-channel independent current sources and voltmeters. It is an optimized system for evaluating stimulation and measurement protocols because of

its fully parallel operations, improved data acquisition speeds, and self-calibration to maintain the performance.

We made a hemispherical phantom using thin plastic sphere. The radius of the hemisphere is 90 mm and height is 92 mm from point **O**. We filled 0.176 Sm^{-1} saline up to 90 mm. The side length of the sliced carrot is 25 mm and it has a cubic shape ($25 \times 25 \times 25$ mm^3). Initially, we measured data without the carrot in the saline phantom. The carrot was placed at the center in the central plane (point **O**′; 46 mm from the point **O**). It was fixed by a very thin wire ($\phi = 0.5$ mm) to minimize the effect from the insulating wire. The cubic carrot was moved over 5 positions along the direction to the electrode number 1 by 12 mm in each step. Conductivity of carrot is 0.026 Sm^{-1} at 10 kHz. In 1, 2, and 3 ring cases, we placed ground electrode at the point of **O**. However, we moved the position of ground electrode to the point **O**" on the top plane of saline for the 10-20 system. All measurements were repeated 64 times (frames) to ensure the measurement accuracy.

III. Results

Fig. 3 shows the $\bar{z}$ values for all 10 electrode geometries, and 8 equal stimulation and measurement patterns based on the cubic target placed in 6 positions in the hemispherical phantom.

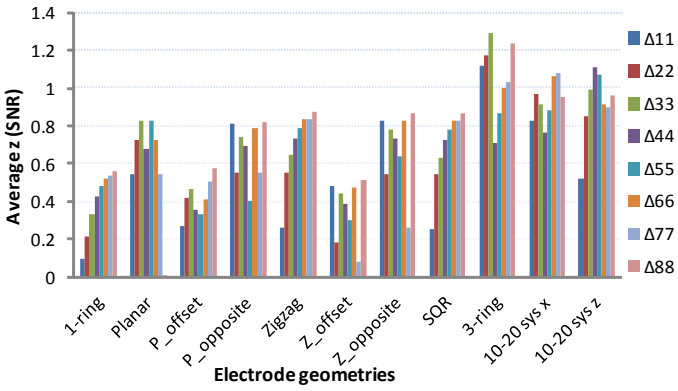

Fig. 3. (i) $\bar{z}$ values of 10 electrode geometries with equal stimulation and measurement patterns based on a target moved horizontally in the central plane.

It can be seen from Fig. 3 that the $\bar{z}$ values vary for different stimulation and measurement patterns. The $\bar{z}$ values increase from $\Delta 11$ to $\Delta 88$ for 1-ring, Zigzag and SQR electrode geometries. Planar-opposite and Zigzag-opposite geometries at $\Delta 11$, as well as Planar-opposite, Zigzag, Zigzag-opposite and SQR at $\Delta 88$ produced higher $\bar{z}$ values. 3-ring electrode geometries and 10-20 system (xspiral and zspiral) produced higher $\bar{z}$ values than 1 and 2 ring electrode configurations.

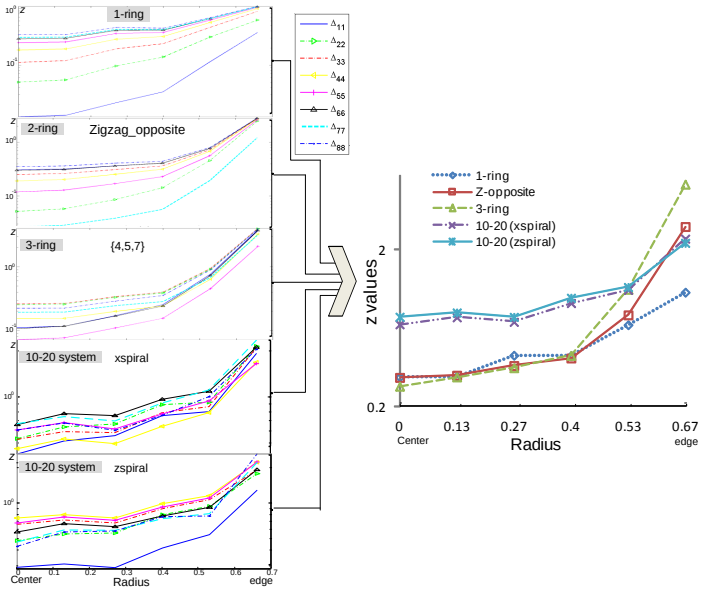

Fig. 4. A graph showing the comparisons of the electrode placement strategies and stimulation patterns (from $\Delta 11$ to $\Delta 88$) for 1, 2, 3 ring electrode geometries, and 10-20 system (x-spiral and z-spiral) with 6 object positions from center towards electrode number 1 (column 1), while selected geometries are compared in column 2 for the best stimulation/measurement patterns (Δsm).

Fig. 4 shows the comparison of 1, 2, 3 ring electrode geometries and 10-20 system (x-spiral and z-spiral) in column 1 for equal stimulation and measurement patterns (from $\Delta 11$ to $\Delta 88$) for 6 object positions moved in the central plane from center towards the electrode number 1 of the hemispherical phantom. In column 1, the simulation is based on the selected best configuration representing for each ring: 1-ring (row 1), 2-ring with 7 electrode placement strategies from planar to square electrode geometries where only Zigzag-opposite is shown (row 2), 3-ring with 5 electrode geometries such as $\{1, 6, 9\}$, $\{3, 5, 8\}$, $\{4, 5, 7\}$, $\{4, 6, 6\}$ where only $\{4, 5, 7\}$ electrode configuration is shown (row 3), 10-20 system with x-spiral (row 4) and z-spiral (row 5). A further comparison was made on the selected electrode geometries with corresponding stimulation and measurement patterns in column 2. 3-ring geometry performed better than 10-20 system for the cubic target placed at the edge, while it has lower z values than 10-20 system for the target placed in the middle and center of the hemispherical phantom.

Fig. 5 shows the comparison of simulation and measurement z values for the target positions of Y=12 and 48 using the 10-20 system with zspiral current driving pattern by applying 8 stimulation patterns (Δs=1 to 8) and adjacent measurement. We assume that noise amplitude is constant for all measurements. Error bar

indicates the measurement error in the figure.

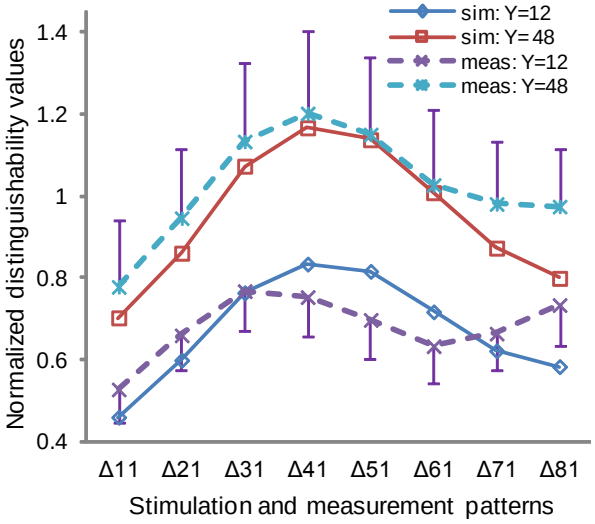

Fig. 5. Comparisons of simulation and measurement based on normalized z values (to maximum) obtained from the 10-20 system with zspiral current driving pattern by applying 8 current patterns (Δs=1 to 8) and adjacent measurement for 2 object positions along Y coordinate of the tank and fixing its position on X in the central plane. Standard errors were taken from standard deviation of measurement voltages. Sim stands for simulation in the caption and meas is for measurement.

It can be seen from Fig. 5 that simulation and measurement results based on normalized z values are in good agreement. Higher distinguishability was obtained for the objects placed on the periphery of the hemispherical phantom for all stimulation and measurement patterns. The $\bar{z}$ and z values show that adjacent electrode approach performed worse than all other patterns. The current injections $\Delta 41$ performed better than all other current patterns. The error is high for the target location close to edge and low for the target at the center.

IV. DISCUSSIONS AND CONCLUSIONS

The objective of this study is to select such an electrode geometry for head stimulation that provides high distinguishability (SNR). We simulated electrode placement strategies, and stimulation and measurement patterns for a hemispherical phantom. We further experimentally evaluated a selected case with a KHU Mark 2 EIT system in single and multi-layer electrode placement strategies. There are a lot of different ways to arrange electrodes and sequences in 3D with two ring and three ring electrodes to give special emphasis or limit a region of interest for impedance measurement.

As shown in Fig. 4, the areas of maximum sensitivity lay on the periphery of the phantom and fall off rapidly towards the center of the hemisphere, so the target positions close to the edge has higher effect on z than the positions middle or central part of the phantom (Fig. 4). Results were strongly influenced by different electrode geometries and stimulation / measurement patterns. Several electrode geometries combined with certain stimulation and measurement patterns produced higher sensitivity to the cubic object placed within the homogenous hemispherical phantom. The stimulation patterns on electrodes located almost opposite side of the phantom produced much higher z values than adjacent stimulation and measurement patterns, which is consistent with the suggestion to adjacent pattern [3].

Investigation (Fig. 4 and Fig. 3) showed that multi-layer electrodes performed better than 1-ring electrodes for 3D EIT with different stimulation and measurement patterns and, 10-20 system of electrode placement is appeared to be the best choice with higher z for different target positions in hemispherical phantom so we recommend it for the head EIT. The experimental results (KHU Mark2) based on 10-20 system with zspiral current driving pattern is in good agreement with the simulation results as shown in Fig. 5. The results suggest that 1-ring electrode placement is a poor design and should be avoided for head imaging.

The 3D electrode placement demonstrated in this study provides high distinguishability (SNR) within the hemispherical phantom which could be subsequently applied to the head especially for the application of cerebral stroke. Although we did not include the effect of the skull for brain imaging, to develop a practical EIT system for head application, optimized electrode placement strategies and good stimulation/measurement patterns should be chosen as suggested in this study to increase sensitivity and distinguishability, which may allow significant contrast between different brain tissues to detect haemorrhagic stroke in the brain for instance.

REFERENCES

[1] B. Brown and A. Seagar, "The sheffield data collection system," *Clin. Phys. Physiol. Meas.*, vol. 8, pp. 91–97, 1987.

[2] L. Fabrizi, A. McEwan, T. Oh, E. Woo, and D. Holder, "An electrode addressing protocol for imaging brain function with electrical impedance tomography using a 16-channel semiparallel system," *Physiol. Meas.*, vol. 30, pp. S85–101, 2009.

[3] A. Adler, P. Gaggero, and Y. Maimaitijiang, "Adjacent stimulation and measurement patterns considered harmful," *Physiological Measurement*, vol. 32, no. 7, p. 731, 2011.

[4] A. Adler and W. Lionheart, "Uses and abuses of eidors: An extensible software base for eit," *Physiol Meas*, vol. 27, p. 25, 2006.

[5] B. Graham and A. Adler, "Electrode placement configurations for 3d eit," *Physiol. Meas.*, vol. 28, pp. S29–44, 2007.